

DIRECT SYNTHESIS OF MoS₂ NANODOTS BY CHEMICAL VAPOR DEPOSITION

VY ANH VUONG AND CHU MANH HUNG [†]

*International Training Institute for Materials Science (ITIMS),
Hanoi University of Science and Technology,
No. 1 Dai Co Viet, Hanoi, Vietnam*

[†]E-mail: mhchu@itims.edu.vn/ hung.chumanh@hust.edu.vn

Received 08 June 2018

Accepted for publication 30 October 2018

Published 15 December 2018

Abstract. *The current work reports a direct synthesis of MoS₂ nanodots by a chemical vapor deposition method. The morphological, crystal structure, and optical properties of the growing MoS₂ are investigated by field emission scanning electron microscopy (FESEM), atomic force microscopy (AFM), X-ray diffraction (XRD), Raman and Photoluminescence (PL) spectroscopy, respectively. High magnification FESEM image reveals a layer of MoS₂ nanodots with the average size of about 10 nm. AFM and XRD data indicate the surface roughness of the nanodot array of about 1.7 nm and the formation of 3R-MoS₂ structure, respectively. Resonance Raman data exhibits the two active E_{2g}¹ and A_{1g} modes corresponding to in-plane vibration of Mo and S atoms centered at 383.3 cm⁻¹ and to out of plane vibration of S atoms located at 407.1 cm⁻¹, respectively. The spacing between two peaks is about 23.8 cm⁻¹, which can be used to evaluate the number of MoS₂ layer. The Raman spectrum also indicates any intensity enhancement of the A_{1g} peak compared to the E_{2g}¹ peak. This result is elucidated through the quantum confinement effect. The PL emission shows a pronounced peak at 505 nm that is significant blue shift compared to thin layer MoS₂. The interpretation of this phenomena is also discussed in detail.*

Keywords: MoS₂, thin layer, nanodots, CVD.

Classification numbers: 81.15.Gh; 62.23.Eg; 81.15.-z.

I. INTRODUCTION

During the past decade, graphene has been attracted much attention among the 2-dimensional (2D) materials owing to their outstanding electronic and optical properties for application to future nanodevices [1,2]. However, graphene has a zero bandgap, which is a major disadvantage to hamper its application to achieve high performance nanoelectronics and optoelectronics devices [2,3]. To complement the lack of the certain bandgap of this 2D material, in recent years, molybdenum disulfide (MoS₂) has received great research interest because of having not only the similar characteristics of graphene, but also a tunable bandgap varying from 1.1 eV to 1.9 eV with respect to a change of thickness from bulk to single layer [4]. It suggests a great potential application to high performance logic devices, integrated circuits, and optoelectronics [5]. Therefore, much effort has been paid to produce the thin film MoS₂ with a controlled layer using both a “top-down” exfoliation and “bottom-up” synthesis [6].

In addition to the thin film type, MoS₂ quasi- and/or quantum dots (QDs) have also received much attention owing to the appearance of quantum confinement effect in this material [7]. It results in the direct bandgap of multi- and mono-layer MoS₂ nanodots are expanded in a range of 2.5 eV to 2.9 eV in comparison with the direct gap of single layer MoS₂ sheet of 1.9 eV [8,9]. This feature allows the MoS₂ nanomaterials being used in a large range of application, including of the novel nanoelectronic and optoelectronic devices. MoS₂ quasi-QDs or nanodots can be synthesized through several ways such as wet grinding assisted co-solvent sonication [10], hydrothermal treatment in combination with bath- and probe- sonication [7, 11], and thermal annealing process of single layer MoS₂ grown by chemical vapor deposition (CVD) [2]. However, these approaches normally include several processes, which make the growth method more complicated. While direct growth of MoS₂ quantum- and/or nano-dots on insulating substrates is an advantage method for future electronic device fabrication, and measurement.

In the current work, a simple and direct synthesis of MoS₂ quasi-quantum dots and/or nanodots using only single CVD growth process is reported. The growing MoS₂ nanodots with the average size of about 10 nm represents characteristics like MoS₂ quantum dots. This is certified through the AFM, XRD, Raman and photoluminescence spectroscopy investigation.

II. EXPERIMENTAL PROCEDURE

Prior to the growth of the MoS₂ nanodots, amorphous SiO₂/Si substrate (the so-called Si substrate) with a typical size of 10 mm × 10 mm × 1 mm was ultrasonically cleaned in acetone and ethanol for 5 minutes, respectively. The substrate was blown dry by a compressed air gun. A Mo thin film of about 3 nm was deposited onto the Si substrate using a rf sputtering technique. For growing the MoS₂, sulfur powder (S, 99%, Xilong scientific Co., Ltd.) and Ar gas were used as a sulfurization and carrier gas sources, respectively. The S powder putting in a ceramic boat and the Mo/SiO₂/Si substrate were placed at the center of zone 1 and zone 2 in the tube furnace, respectively (as shown in Fig. 1). Zone 2 was set at 800°C with a heating rate of 15°C/min. After a certain time, the temperature of zone 1 was increased to 150°C with a similar heating rate of 15 °C/min. It ensures that the temperatures at two zones will reach the desired values at the same time. Ar gas flow was then switched on with the rate of 100 standard cubic centimeters per minute (sccm) and the direction as shown in Fig. 1. The sulfurization process of the Mo film

coated Si substrate was carried out for 15 min at 800°C with the pressure of 310 mTorr. After the sulfurization process, the tube furnace was cooled down to room temperature (RT).

The morphology of thin-layer MoS₂ nanodots was investigated by field emission scanning electron microscope (FESEM; JEOL JSM-7600F) and atomic force microscopy (AFM). Crystal structure of the MoS₂ nanodots was characterized by X-ray diffraction technique using Cu-K_α radiation ($\lambda = 0.15418$ nm). Raman spectroscopic system (Renishaw, InVia) with 633 nm wavelength excitation laser was employed to study the vibrational modes in the MoS₂ structure. Photoluminescent properties of the thin-layer MoS₂ nanodots were investigated by using 325 nm He-Cd laser (Kimmon Koha).

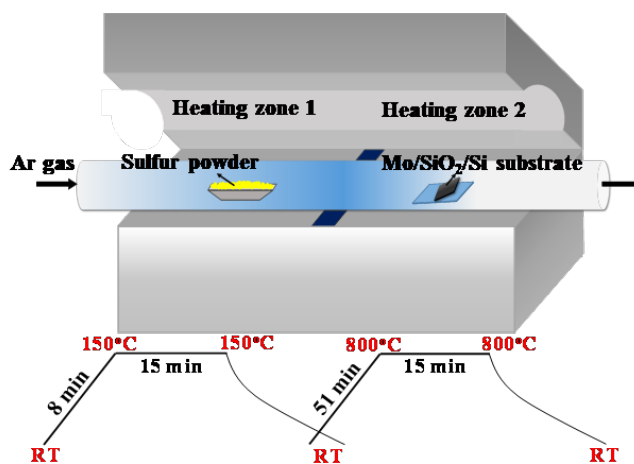


Fig. 1. Schematic illustration for the deposition of MoS₂ nanodots using CVD system.

III. RESULTS AND DISCUSSION

Figure 2(a) shows a low magnification FESEM image of the MoS₂ nanodots formed through the sulfurization process of Mo thin film deposited on the Si substrate. It represents a layer-like MoS₂ nanodots on the whole captured area. Size of the nanodots seems not very uniform. It can be seen more obviously at higher magnification SEM image in Fig. 2(b). The inset of Fig. 2(a) reveals the actual Si substrates before (on the right) and after (on the left) the sulfurization process. With only few nanometers of Mo film deposited on the SiO₂/Si substrate the color of the substrate surface is similar to the surface of SiO₂/Si substrate. On the other hand, the color of the sample after sulfurization process is relatively different with the one of Mo/SiO₂/Si substrate. It was changed from violet color to dark blue color, which is similar with the color of thin layer MoS₂ grown by CVD method [12–14].

Fig. 2(b) displays a higher magnification SEM image of the MoS₂ nanoparticle array. At this magnification, we clearly see that the layer is not a thin film type. It involves MoS₂ nanodots with the size changing from 3 to a few tens of nanometers. The average size of the nanodots is rather small, which results in the quantum confinement effect in the sample. This will be discussed in more detail in the following section. Formation of nanodots that can be attributed to

the sulfurization of ultra-thin Mo film deposited on the substrate. Because of high heating rate (15°C/min) to reach high sulfurization temperature (800°C), the shrinkage of Mo thin film occurs fast and suddenly. Therefore, it can be seen a formation of many nano-islands and/or cracks on the FESEM image.

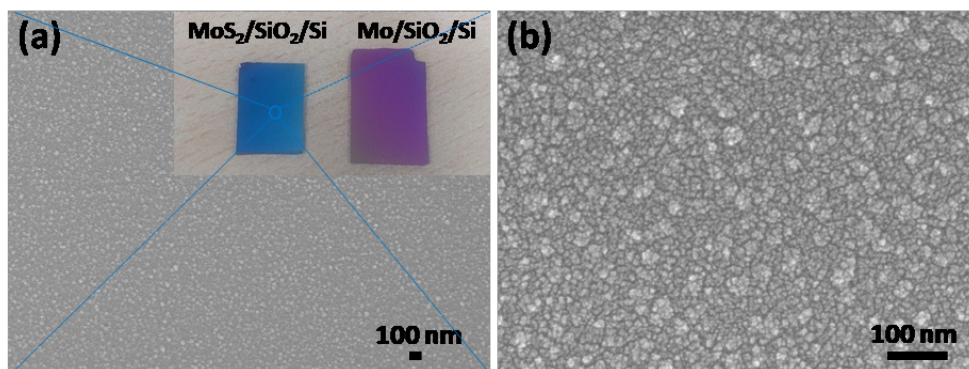


Fig. 2. (a) low magnification FESEM image of the MoS₂ nanodots, the inset is the Si substrates before (on the right) and after (on the left) the sulfurization process. (b) high magnification FESEM image of the MoS₂ nanodots sample.

The morphology of the MoS₂ nanodot array was also studied through the AFM measurement. Fig. 3(a) reveals an AFM image of the MoS₂ nanodots, the surface is rather uniform over large scan area with the roughness of about 1.7 nm. The crystal structure of the MoS₂ nanodots was characterized through X-ray diffraction as shown in Fig. 3(b). Normally, the XRD data of the bulk or thick-layer MoS₂ show highest intensity peaks at $2\theta = 14.4^\circ$, 39.56° , and 49.8° , which correspond to the (002), (103), and (105) planes, respectively. However, Li *et al.* have already indicated that these peaks could be reduced in intensity or even disappeared when the MoS₂ is ultra-thin or existing under nano/quantum dot type [15]. For example, in the case of nanodots, which are very small and thin, resulting in no constructive interference from aligned crystal planes, and therefore no signals or peaks appeared on the XRD pattern [15, 16]. The XRD pattern of our MoS₂ reveal any diffracted peaks for (002), (103), and (105) planes, confirming that the synthesized MoS₂ material is nanodot type, which is in agreement with the result of MoS₂ nanodots grown by an exfoliation method [15, 16]. The peak at $2\theta = 55.4^\circ$ can be originated from the diffraction of the Si substrate corresponding to (311) plane [17], not from the sample.

In order to investigate the vibrational modes of the deposited MoS₂, Raman spectroscopic measurement was carried out with 633 nm excitation laser, which is in resonance with the direct band gap of MoS₂ (~ 1.96 eV) at the K point. Fig. 4(a) shows the Raman spectrum of the MoS₂ nanodots. Inset is an optical image of the MoS₂ sample, showing a center position where the Raman spectrum was recorded. Raman spectra taken on several positions represent similar results (data are not shown here). A representative spectrum indicates two prominent Raman modes (E_{2g}^1 and A_{1g}) of the MoS₂. As depicted in Fig. 4(b), the E_{2g}^1 mode is an in-plane optical vibration of Mo and S atoms; while the A_{1g} mode corresponds to out-of-plane optical vibration of the S atoms [18].

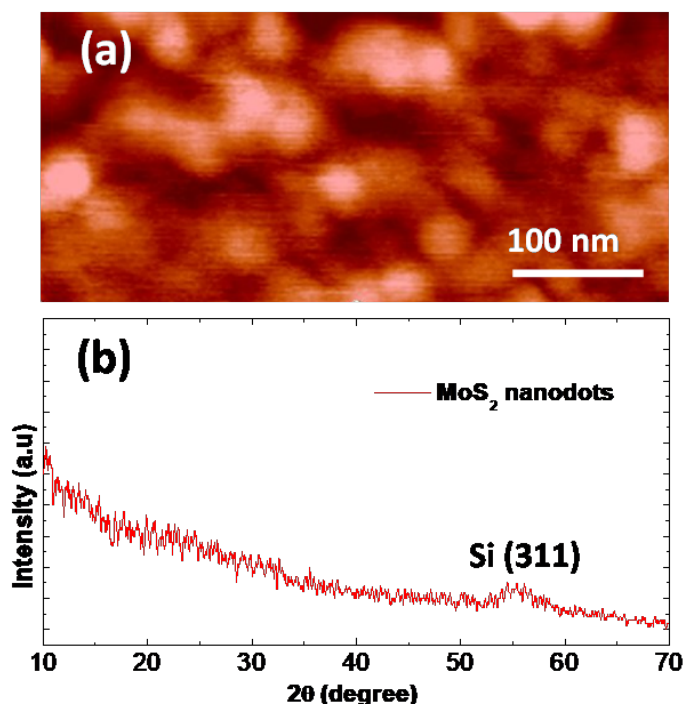


Fig. 3. (a) AFM image of the growing MoS₂ nanodots and (b) XRD pattern of the MoS₂ nanodots grown by CVD method.

In the resonance condition, the A_{1g} mode intensity is normally much higher than the E_{2g}^1 peak intensity [19, 20]. It can be attributed to d_{z^2} orbitals of Mo atoms, which is related to final state of direct electronic transition at K point, is aligned along the same oscillating direction of A_{1g} mode. Thus, it will result in a strong electron-phonon coupling along this direction [19–21]. However, the Raman spectrum of the MoS₂ in current work shows any enhancement of the A_{1g} peak intensity with respect to the E_{2g}^1 intensity. It means that the coupling between the electron transition and the A_{1g} mode phonon is weak at K point, which can be attributed to the increased transition energy at K point owing to the quantum confinement effect along the c -axis [19, 22]. Raman result indicated an existence of the quantum confinement in the MoS₂ nanodots, this is consistent with the photoluminescence result.

Apart from these two modes, the spectrum also reveals an existence of other peaks at 419, 460, and 532 cm^{-1} . The mode of 419 cm^{-1} at a shoulder of the A_{1g} peaks belongs to Raman-inactive mode (B_{1u}), which is generated from the scattering process of a transverse optical phonon and longitudinal quasi-acoustic phonon [19]. The 2LA(M) peak at ~ 460 cm^{-1} is assigned to a second-order process involving the longitudinal acoustic phonons at M point [19, 23] (the first LA(M) mode at 230 cm^{-1} is not shown in the graph). Finally, the peak at 532 cm^{-1} is a vibrational mode of the Si substrate.

To further study the optical properties of the MoS₂ nano-particles, the PL measurement was carried out using a 325 nm laser excitation. Fig. 5 reveals a PL spectrum of the MoS₂ nanodots. It

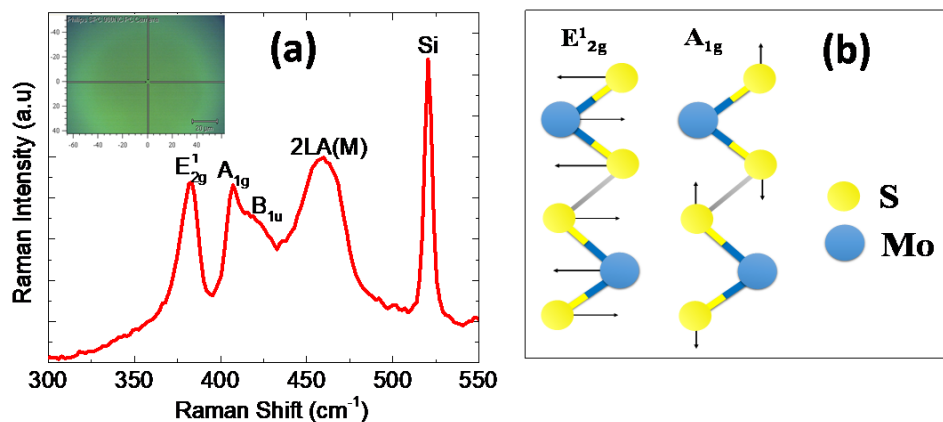


Fig. 4. (a) Raman spectrum of the MoS₂ nanodots using a 633 nm excitation wavelength. Inset is an optical image of the MoS₂ sample. (b) Visualization of Raman active modes (E_{2g}^1 and A_{1g}).

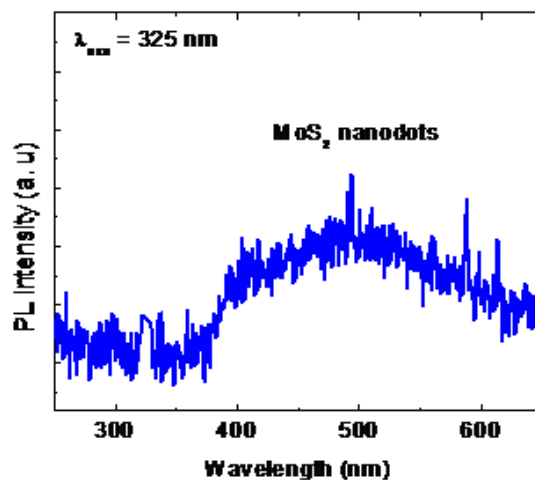


Fig. 5. PL spectrum of the MoS₂ nanodots excited with the 325 nm wavelength laser.

shows a broad peak centered at ~ 505 nm together with a shoulder centered at ~ 410 nm, which are strongly blue shifted in comparison with the single- or multi-layer MoS₂ [24,26]. These peaks are in agreement with the ones observed in the low-dimensional exfoliated MoS₂ nanoflakes [27] as well as in the MoS₂ quantum dots [2, 11, 28]. Jian Zhen Ou *et al.* explain the appearance of these peaks, which are attributed to the hot PL from the K point of the Brillouin zone [27]. On the other hand, other reports elucidate that the existence of peaks at the blue region is due to the quantum confinement effect [2, 11, 28]. In these reports, the particle size is in a range of 2 to 8 nm. While the MoS₂ nanodots in the current work has also an average size that is comparable to the one of previous reports. Therefore, the origin of the MoS₂ PL peak in our work is related to

the quantum confinement effect. This finding is in good agreement with the Raman result above. It suggests that the growing MoS₂ in the current work shows the characteristics of its thin film and also the quantum confinement effect.

IV. CONCLUSION

In summary, the MoS₂ nanodots were successfully grown by a direct CVD process. Optical image obviously indicated a different color on the surface of the sample before and after MoS₂ growth. Low and high magnification SEM and AFM images showed clearly a MoS₂ nanodots with a size of 3 to a few tens of nanometers with the surface roughness of about 1.7 nm. XRD data affirmed the synthesized MoS₂ having very thin and small nanodot shape. Raman spectroscopy result revealed two characteristic vibration modes E_{2g}^1 and A_{1g} of the MoS₂. Interestingly, the peak intensity of the A_{1g} mode was slightly smaller than the one of the E_{2g}^1 mode, which could be explained through the quantum confinement effect in the MoS₂ nanodots along the c-axis. This interpretation was also supported by the PL result.

ACKNOWLEDGMENTS

This work was financially supported by Hanoi University of Science and Technology under project number T2017-TT-006. We would like to thank associate professor Nguyen Ngoc Trung, Dr. Luu Thi Lan Anh (SEP, HUST) and Dr. Pham Nguyen Hai (HUS-VNU) for their help in Raman and AFM measurements, respectively.

REFERENCES

- [1] M. Liu, X. Yin, E. Ulin-Avila, B. Geng, T. Zentgraf, L. Ju, F. Wang, X. Zhang, *Nature* **474** (2011) 64.
- [2] S. J. Park, S. W. Pak, D. Qiu, J. H. Kang, D. Y. Song, E. K. Kim, *J. Lumin.* **183** (2017) 62.
- [3] X. Li, W. Cai, J. An, S. Kim, J. Nah, D. Yang, R. Piner, A. Velamakanni, I. Jung, E. Tutuc, S.K. Banerjee, L. Colombo and R.S. Ruoff, *Science* **324** (2009) 1312.
- [4] J. Park, N. Choudhary, J. Smith, G. Lee, M. Kim and W. Choi, *Appl. Phys. Lett.* **106** (2015) 012104.
- [5] X. Ling, Y. Lee, Y. Lin, W. Fang, L. Yu, M. S. Dresselhaus and J. Kong, *Nano Lett.* **14** (2014) 464.
- [6] X. Wang, H. Feng, Y. Wu and L. Jiao, *J. Am. Chem. Soc.* **135** (2013) 5304.
- [7] X. Zhu, J. Xiang, J. Li, C. Feng, P. Liu and B. Xiang, *J. Colloid Interface Sci.* **511** (2018) 209.
- [8] L. Lin, Y. Xu, S. Zhang, I. M. Ross, A. C. M. Ong and D. A. Allwood, *ACS Nano* **7** (2013) 8214.
- [9] X. Lu, R. Wang, L. Hao, F. Yang, W. Jiao, P. Peng, F. Yuan and W. Liu, *Phys. Chem. Chem. Phys.* **18** (2016) 31211.
- [10] G. U. Siddiqui, J. Ali, K. H. Choi, Y. Jang, K. Lee, *J. Lumin.* **169** (2016) 342.
- [11] Z. Gan, Q. Gui, Y. Shan, P. Pan, N. Zhang, L. Zhang, *J. Appl. Phys.* **120** (2016) 104503.
- [12] M. Park, Y. J. Park, X. Chen, Y. K. Park, M. S. Kim, J. H. Ahn, 2556.
- [13] S. Wang, M. Pacios, H. Bhaskaran, J. H. Warner, *Nanotechnology* **27** (2016) 085604.
- [14] N. Choudhary, J. Park, J. Y. Hwang and W. Choi, *ACS Appl. Mater. Interfaces* **6** (2014) 21215.
- [15] B. Li, L. Jiang, X. Li, P. Ran, P. Zuo, A. Wang, L. Qu, Y. Zhao, *Sci. Rep.* **7** (2017) 11182.
- [16] T. P. Nguyen, W. Sohn, J. H. Oh, H. W. Jang, S. Y. Kim, *J. Phys. Chem. C* **120** (2016) 10078.
- [17] L. Tian, E. Fathi, R. S. Tarighat and S. Sivoththaman, *Semicond. Sci. Technol.* **28** (2013) 105004.
- [18] G. Plechinger, J. Mann, E. Preciado, D. Barroso, A. Nguyen, J. Eroms, C. Schüller, L. Bartels and T. Korn, *Phys. Rev. Lett.* **29** (2014) 064008.
- [19] H. Li, Q. Zhang, C.C.R. Yap, B.K. Tay, T. H. T. Edwin, A. Olivier and D. Baillargeat, *Adv. Funct. Mater.* **22** (2012) 1385.
- [20] R. Coehoorn, C. Haas and R. A. de Groot, *Phys. Rev. B* **35** (1987) 6203.
- [21] G. L. Frey, R. Tenne, M. J. Matthews, M. S. Dresselhaus and G. Dresselhaus, *Phys. Rev. B* **60** (1999) 2883.

- [22] A. Splendiani, L. Sun, Y. Zhang, T. Li, J. Kim, C.-Y. Chim, G. Galli, F. Wang, *Nano Lett.* **10** (2010) 1271.
- [23] B. C. Windom, W. G. Sawyer, D. W. Hahn, *Tribol. Lett.* **42** (2011) 301.
- [24] D. J. Late, Y. K. Huang, B. Liu, J. Acharya, S. N. Shirodkar, J. Luo, A. Yan, D. Charles, U. V. Waghmare, V. P. Dravid and C. N. R. Rao, *ACS Nano* **7** (2013) 4879.
- [25] C. Lunceford, E. Borcean, J. Drucker, *Cryst. Growth Des.* **16** (2016) 988.
- [26] S. Wang, Y. Rong, Y. Fan, M. Pacios, H. Bhaskaran, K. He, J. H. Warner, *Chem. Mater.* **26** (2014) 6371.
- [27] K. Kalantar-zadeh, *Nano Lett.* **14** (2014) 857.
- [28] H. Dong, S. Tang, Y. Hao, H. Yu, W. Dai, G. Zhao, Y. Cao, H. Lu, X. Zhang and H. Ju, *Appl. Mater. Interfaces* **8** (2016) 3107.